

How synchronized human networks escape local minima

Received: 25 September 2023

Accepted: 16 October 2024

Published online: 28 October 2024

 Check for updates

Elad Shniderman¹, Yahav Avraham^{2,3}, Shir Shahal^{2,3}, Hamootal Duadi^{2,3}, Nir Davidson⁴ & Moti Fridman^{2,3} ✉

Finding the global minimum in complex networks while avoiding local minima is challenging in many types of networks. In human networks and communities, adapting and finding new stable states amid changing conditions due to conflicts, climate changes, or disasters, is crucial. We studied the dynamics of complex networks of violin players and observed that such human networks have different methods to avoid local minima than other non-human networks. Humans can change the coupling strength between them or change their tempo. This leads to different dynamics than other networks and makes human networks more robust and better resilient against perturbations. We observed high-order vortex states, oscillation death, and amplitude death, due to the unique dynamics of the network. This research may have implications in politics, economics, pandemic control, decision-making, and predicting the dynamics of networks with artificial intelligence.

Human interactions form complex networks of connections between the members of the networks. Synchronizing human networks can happen spontaneously^{1,2} or intentionally^{3,4}. The synchronization of the network is essential for coordinating ideas^{5,6}, and the well-being of its members^{7–9}, and is seen in other organisms as well^{10–12}. Understanding the dynamics of human networks has implications for politics, economics, social sciences, and pandemic control. The topology of human networks determines if the network will be able to synchronize¹³, who is most probable to become a leader¹⁴, which decision the humans in the network are more likely to make^{5,15}, and how stable is the network to small perturbations^{16–18}.

The synchronization dynamics of networks can be analyzed in terms of an effective potential landscape in which the system evolves^{19,20}. To reach the fully synchronized state, which is the global minimum of this potential landscape, a human network must avoid getting trapped in local minima, where not all humans are synchronized^{19–24}. The concept of escaping local minima is significant in various systems including biological systems²⁵, physical systems²⁶, and deep neural network learning^{27,28}. It also has implications for increased stability in other types of networks²⁹, and optimization problems in spin-glass dynamics³⁰.

Human networks can reach synchronization by finding unique solutions that are more stable to small perturbations compared to other networks due to the human ability to focus on some inputs while ignoring other inputs³¹. However, it is still unclear how human networks reach these stable solutions, what the network dynamics that lead to it are, and in particular, how the human network escapes local minima. In addition, previous studies focus on local frustration where some nodes are in a state of frustration^{31,32}, while in real-life networks, many networks have global frustration due to their topology. This type of frustration is not local at a specific position in the network but emerges when the entire network tries to synchronize.

We study how human networks find and reach the stable solution, we study the network dynamics during the search for the stable solution, and the different methods the network is using to escape local minima. We focus on networks where each node has a single input and the frustration is global and rises from its topology. Our investigated networks are the unidirectional coupled rings that serve as basic building blocks and motifs to any complex network, together with the bidirectional rings³¹. We study the rhythmic behavior of humans since it can reveal aspects of human network dynamics that are usually hard to identify³³. Human synchronization in general and

¹Departments of Humanities and Arts, Technion - Israel Institute of Technology, Haifa, Israel. ²Faculty of Engineering, Bar Ilan University, Ramat Gan, Israel.

³Institute of Nanotechnology and Advanced Materials, Bar Ilan University, Ramat Gan, Israel. ⁴Department of Physics of Complex Systems, Weizmann Institute of Science, Rehovot, Israel. ✉ e-mail: mordechai.fridman@biu.ac.il

specifically rhythmic behaviors are critical in fields like organizational behavior, management, and policy-making^{34–37}.

In this paper, we study the synchronization dynamics of human networks with closed-ring topology and unidirectional time-delayed coupling of violin players (Fig. 1a). Such a network has a complex potential landscape with well-defined local and global minima^{18,38,39} that we can tune and control in real-time. We prepare the system in a global minimum (fully synchronized) state and then adiabatically (slowly) transform the potential landscape by tuning the coupling delay time between the players such that this state becomes a local minimum. We then study in detail how the system escapes this local minimum into the new fully synchronized global minimum by measuring each player's amplitude, tempo, and phase and identifying which player is following which.

We show that humans can escape local minima by self-tuning local properties of the networks such as their tempo, amplitude, and the coupling strength between players. The ability to tune these parameters dramatically changes the network's dynamics and has implications for other networks where each node has decision-making abilities⁴⁰. We are studying here basic network motifs that have global frustration, these motifs are the building blocks of complex networks^{41,42}, and the dynamics of complex networks are dictated by the dynamics of the motifs^{43,44}. We numerically demonstrate the dynamics of the motifs in large random networks in Supplemental Materials Section S4 and generalize our findings into complex two-dimensional networks in Supplemental Materials Section S3.4.

Our system with coupled violin players is schematically shown in Fig. 1a³¹. The violin players cannot see or hear the others apart from the audio signal they receive through their headphones. The sound of each player is connected to a control system that receives the audio signal from each player and distributes it to other players. The control system

provides a tunable, programmable, and accurate real-time control of the network connectivity (who is connected to whom) the strength of the coupling, and the delay of the coupling between the players. We define the coupling strength as the volume each player is hearing its neighbors compared to the volume of its violin. The players repeat the music phrase shown in Fig. 1b, and are instructed to synchronize with what they hear. In this study, we set the players' network as a unidirectional ring, so each player hears only a single neighbor with periodic boundary conditions, illustrated in Fig. 1a for $N=6$ players. We performed measurements also with different numbers of players including $N=2, 3, 4, 5, 6, 7, 8$, and 16. We measure the note each player is playing as a function of time, and accordingly, obtain the phase $\varphi(t)$ of the player, where $\varphi=0$ denotes that the player is playing the beginning of the musical phrase, and $\varphi=2\pi$ denotes that the player is at the end of the musical phrase of duration T ³¹. Detailed experiment descriptions are presented in Supplemental Materials Section S2.

Each experiment starts with zero time-delay $\Delta t=0$ between all players with coupling strength sufficiently high³¹ to ensure that all players are synchronized in-phase (i.e. playing the same note at the same time, see Fig. 1b). Then, we increase Δt linearly with time as $\Delta t=t/30$. When Δt exceeds nT/N , where n is an integer number, the in-phase state becomes a local minimum and the global minimum solution is a vortex state, where each player has identical delay compared to its neighbor, satisfying the periodic boundary conditions (see Fig. 1b). The players must then leave their in-phase state and find the vortex state. The n parameter denotes the order of the vortex which is stable³⁹. For zero vortex order, $n=0$, the system is at an in-phase state of synchronization, illustrated at the top of Fig. 1b. When $n=1$, we are at the first vortex order, in which adding the delay between the players is equal to 2π , illustrated at the bottom of Fig. 1b. For higher vortex orders, adding the players' delay equals to higher multiples of 2π .

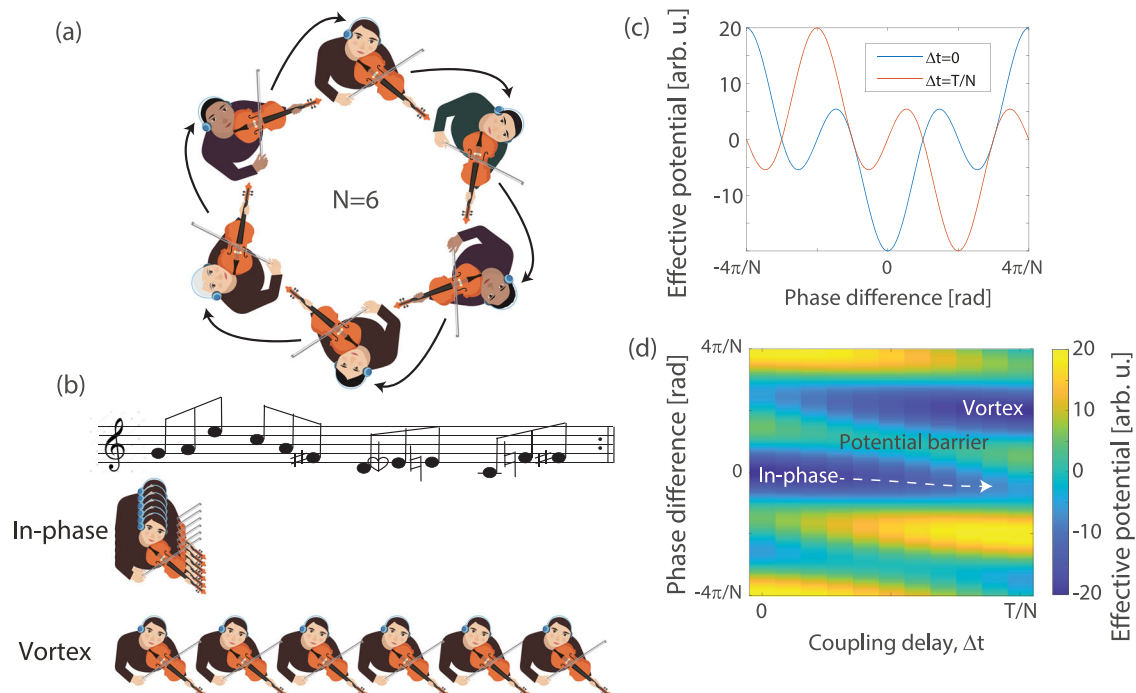


Fig. 1 | Coupled violin players on a unidirectional ring network, where each player is hearing only the player on its right with a controllable delayed coupling. a Schematic of $N=6$ unidirectional coupled players. **b** The musical phrase the players are periodically repeating illustrates the two possible states of synchronization: the in-phase state where all the players are playing the same note at the same time, and the vortex state, where due to the delay between the players, each player is playing a different note. **c** The effective potential (defined in section

2.1) of the system as a function of the phase difference between the players for two values of delay Δt . For $\Delta t=0$, the minimum potential is at zero phase difference, indicating an in-phase state of synchronization. For $\Delta t=T/N$, the minimum potential is at $2\pi/N$ indicating a vortex state and the in-phase state becomes a local minimum, protected by a potential barrier. **d** Effective potential map as a function of the phase difference and delayed coupling between the players.

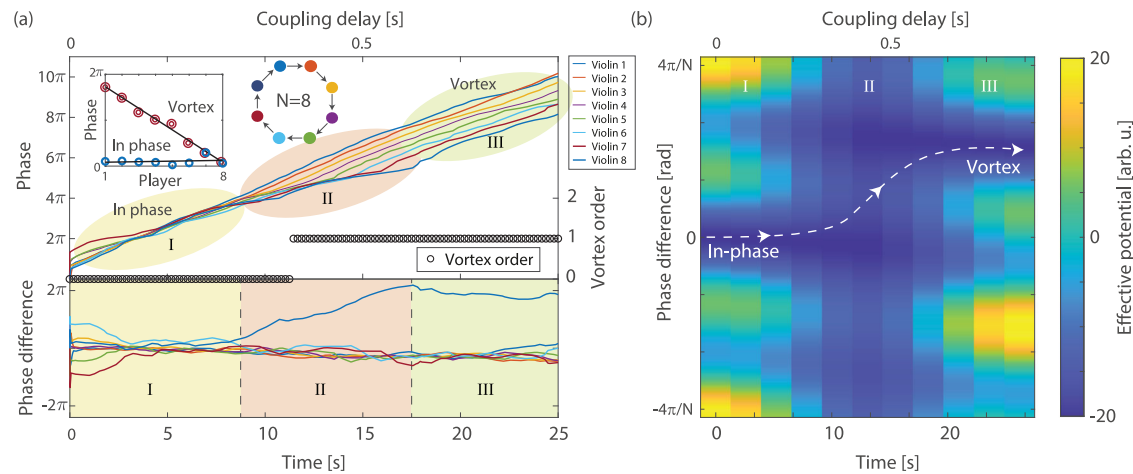


Fig. 2 | Coupled $N = 8$ players situated on a ring in a unidirectional coupling, according to the inset scheme, starting from an in-phase state of synchronization and finding the vortex state. **a (top) Measured phase of each player as a function of time as we increase the coupling delay between the players. Each color denotes the phase of a player according to the inset scheme. Black circles denote the vortex order of the system as a function of time. (bottom) The difference between the phase of each player and the phase of its delayed neighbor. (inset) The**

phase of all players in a state of in-phase synchronization (stage I, blue circles) and the phase of all players in a vortex state (stage III, red circles). **b** The effective potential of the system as a function of time and coupling delay. In stage II the effective coupling strength is reduced (see text) thus eliminating the potential barrier between the in-phase and the vortex states to enable the system to reach the global minimum vortex state. The trajectory of the system is denoted by the white dashed curve.

The dynamics of the coupled violin players performing a periodic rhythm can be analyzed by the Kuramoto model^{45–47} which describes an over-damped motion of coupled phase oscillators in an effective potential^{19,20,23,24}. The derivation of the Kuramoto effective potential is presented below in Section 2.1. An effective potential is a powerful tool for predicting the dynamics of a coupled system and analyzing its stability^{19,20,23,24}. Figure 1c depicts two representative effective potentials, for $\Delta t = 0$ and $\Delta t = T/N$, respectively, as a function of the phase difference between coupled players. For $\Delta t = 0$, the global minimum potential is at zero phase difference between coupled players, corresponding to the in-phase synchronization state. For $\Delta t = T/N$, the global minimum of the potential is at a phase difference of $2\pi/N$, corresponding to a vortex state of synchronization, while the in-phase state becomes a local minimum.

Figure 1d presents the effective potential as a function of Δt . The dashed line denotes the system trajectory in the phase space as the delay increases from $\Delta t = 0$. The system starts from the in-phase state and for the system to reach the emerging global minimum vortex state, it must overcome a potential barrier. Here, we present and analyze four types of dynamics in human networks for overcoming this potential barrier and escaping the local minimum into the global one.

In the first dynamics, some of the players ignore the signals they receive, thereby reducing the effective coupling strength to their neighbor. Then, they can freely spread their phase to reach the vortex state (see section “Spreading the phase”). In the second, the players are slowing down their tempo so the in-phase state remains the global minimum for arbitrarily large delays (see section “Slowing the tempo”). In the third, the players further slow down until everyone plays the same note indefinitely. This state, known as oscillation death⁴⁸, is a stable synchronized solution regardless of the delay between the players. The players then spontaneously emerge from the oscillation death directly into the globally stable vortex state (see section “Oscillation death and amplitude death”). In the fourth, some of the players stop playing (i.e. reduce their amplitude to near zero). In this state, known as amplitude death, the network topology changes into an open ring, where the local minima and its potential barrier disappear. Thus, enabling the other players to find the vortex state (see section “Oscillation death and amplitude death”).

We observed these four distinct strategies to escape local minima at all network sizes from $N = 2$ up to $N = 16$ players. While representing different emerging strategies to overcome barriers and reach stable minima, they all rely on the unique ability of human players to adjust their playing amplitude and tempo and change the effective coupling strength between them by ignoring frustrating inputs. More results are shown in the Supplemental Materials in Section S3.

Results

Spreading the phase

The first dynamic we observe is when the players are spreading their phases to escape from the in-phase local minimum into a vortex-phase state global minimum. This dynamic is enabled by the players’ ability to reduce the coupling between them until they find a stable state.

Figure 2a(top) presents the measured phase of $N = 8$ players situated on a ring with unidirectional coupling as a function of time t and delay $\Delta t = t/30$. Fig. 2a(bottom) presents the measured phase difference between each player and its delayed neighbor. As seen, during the first 3 seconds all phase difference converges to near zero, indicating that all players are synchronized in phase, and remain so until $t = 8$ s. This first stage is marked as stage I. The average phase of each player during this stage, presented as the blue circles in the inset of Fig. 2a, confirms that all the players have nearly the same phase. When the delay is further increased, one of the players starts to ignore its neighbor, indicated by the linearly increasing blue curve in the phase difference in Fig. 2a(bottom). Thus, the other players can freely change their phase to follow the increasing delay between them. This is marked as stage II. The phase of the players spread until reaching a total phase difference of 2π between the first and the last player, thus forming a stable vortex solution in the first vortex order³⁹, shown as the black circles in Fig. 2a. This vortex solution remains stable as the delay is further increased, indicated by a constant phase difference between all coupled neighbors (marked as stage III). The average phase of all players in stage III is shown as red circles in the inset of Fig. 2a, and verifies the expected linear phase of the vortex state.

Following^{19,20,23,24}, we use the Kuramoto model for N oscillators on a ring with unidirectional time-delayed coupling^{45–47} and uniform distributed random frequency ω_n to introduce an effective potential whose local and global minima dictate the players’ dynamics.

The phase of each oscillator $\varphi_n(t)$ follows:

$$\frac{\partial \varphi_n(t)}{\partial t} = \omega_n + \kappa \sin(\varphi_{n+1}(t - \Delta t) - \varphi_n(t)), \quad (1)$$

with κ , and Δt denoting the strength and delay of the coupling. The periodic boundary conditions, $\varphi_{i+N} = \varphi_i$ dictate $\sum_{n=1}^N \Delta \varphi_n = 0$, where $\Delta \varphi_n(t) = \varphi_{n+1}(t) - \varphi_n(t)$. Assuming uniformity $\Delta \varphi_n = \Delta \varphi$, we obtain:

$$\frac{\partial \Delta \varphi(t)}{\partial t} = - \frac{\partial V(\Delta \varphi)}{\partial \Delta \varphi}. \quad (2)$$

where the effective potential governing the dynamics of the system is:

$$V(\Delta \varphi) = - \Omega \Delta \varphi - \frac{\kappa}{N-1} \cos((N-1)\Delta \varphi + \omega \Delta t) - \kappa \cos(\Delta \varphi - \omega \Delta t), \quad (3)$$

where $\Omega = \sum(\omega_{n+1} - \omega_n)/N$, and $\omega = \sum \omega_n/N$. The same derivation holds for non-uniform phase differences, as long as two adjacent phase differences are similar. The detailed analytical derivation is presented in Supplemental Materials Section S1.1.

The calculated effective potential for constant tempo is shown in Fig. 1d as a function of Δt and $\Delta \varphi$. For $\Delta t = 0$ it reveals a global minimum at $\Delta \varphi = 0$, where all oscillators have the same frequency and phase, namely, an in-phase state of synchronization. However, when the delay increases beyond $\omega \Delta t > \pi/(2N)$, the $\Delta \varphi = 0$ becomes a local minimum and the vortex state emerges as a new global minimum at $\Delta \varphi = -2\pi/N$. Between the in-phase state and the vortex state, there is a potential barrier. Therefore, increasing the delay adiabatically (slowly), so the network remains in the in-phase state of synchronization, transfers the system to a local minimum.

To account for the players' dynamics observed in Fig. 2, we assume that the coupling strength in stage II is reduced by the player's tendency to ignore frustrating inputs. Specifically, we assume $\kappa(t) = \kappa(t=0) \cos^2(\Delta t N \pi / T)$. The resulting modified effective potential is shown in Fig. 2b. The dashed curve follows the system trajectory in the phase space. The system starts in an in-phase state of synchronization and as the delay increases, the coupling drops leading to a lower potential barrier. Thus, the system can evolve into the vortex state. Finally, the coupling increases back to its original value $\kappa(t=0)$.

When the delay between the players is further increased, the first-order vortex becomes unstable and the next-order vortex becomes stable. We observed such multiple transitions to higher-order vortex states with $N=16$ coupled violin players on a unidirectional ring. The measured phases of all the players together with the vortex order of the network are shown in Fig. 3a. In the inset, we show the phase of the players at four representative times, 1.5, 13.5, 24, and 34 seconds, with vortex orders $n = 0, 1, 2$, and 3 , respectively. As the players' phases spread over a wider range, the network reaches a higher vortex state, denoted by a higher vortex order. We also calculate the effective potential as a function of time, again assuming $\kappa(t) = \cos^2(\Delta t N \pi / T)$, showing how the system can evolve from the in-phase to each order of vortex.

Slowing the tempo

The second dynamic we observe is the slowing down of the players' tempo as an alternative strategy to maintain a stable in-phase synchronization state in the presence of delayed coupling⁴⁹. The measured phase results as a function of time for six coupled players are shown in Fig. 4a. From these results, we evaluate the tempo of the players by calculating the average derivative of the phase. As seen, the initial (natural) tempo of 60 bpm slows down significantly for long delay times reaching about 6 bpm for $\Delta t > 1$ s. This slowing down lets

players maintain the in-phase state of synchronization by keeping the coupling delay small relative to the tempo.

To quantitatively analyze the tempo slowing, we resort again to the Kuramoto model⁴⁵⁻⁴⁷. Assuming $\Delta t < T/N$, we can expand $\varphi_n(t - \Delta t) \approx \varphi_n(t) - \Delta t \partial \varphi_n / \partial t$ and $\sin(\alpha) \approx \alpha$ to obtain from Eq. (1) the phase difference as a function of time for $\Delta \varphi_{N-1}$:

$$\frac{\partial \Delta \varphi(t)}{\partial t} = \frac{\Omega - N \kappa \Delta \varphi}{1 - (N-1) \kappa \Delta t}, \quad (4)$$

where Ω is the average tempo difference between the players. Then we obtain,

$$\frac{\partial \varphi(t)}{\partial t} = \frac{\omega}{1 + \kappa \Delta t}, \quad (5)$$

where $\varphi = \sum \varphi_n / N$ is the average phase of all oscillators. Thus, the tempo of the coupled oscillators slows down as long as the players stay phase-locked, ensuring that the condition $\Delta t < T/N$ is satisfied and indicating that our assumptions are valid. Using Eq. (5), to fit the measured tempo (blue curve in Fig. 4a) yields excellent agreement, where the fit parameters $\omega = 0.29$ Hz and $\kappa = 0.63$ are consistent with our system. The detailed analytical derivation is presented in the Supplemental Materials Section S1.2.

Next, We perform numerical simulations of the Kuramoto model (Eq. (1)) for six coupled players with a coupling strength of $\kappa = 0.6$. The calculated phase of all the players as a function of time/delay together with the average tempo are shown in Fig. 4b. As evident, the exact numerical simulations agree with the measured experimental results as well as with the analytical approximation of Eq. (5) (blue curve in Fig. 4b).

Finally, We calculate the effective potential as a function of time with the tempo obtained from Eq. (5). As evident, the in-phase state of synchronization remains the global minimum even though the coupling delay increases. Therefore, the system follows the dashed line and remains in the in-phase synchronization state for all coupling delays.

Oscillation death and amplitude death

In this section, we present two additional mechanisms that have been observed in other networks on coupled nonlinear oscillators: oscillation death⁴⁸ and amplitude death⁵⁰, and show how both enable the human network to escape from a local minimum (in-phase synchronization) into a global one (vortex state).

When the tempo slows too much, the players can get stuck in a state of oscillation death⁴⁸ where all the players are playing the same note indefinitely, thereby maintaining a degenerate form of synchronization. Representative results of such oscillation death for four coupled violin players are shown in Fig. 5a. The four players are slowing down their tempo, and after 40s they all play the same note for 20 seconds. Then, the players spontaneously revive the oscillation when one of the players stopped following its neighbor. Reviving oscillations after oscillation death typically requires external perturbation to the system⁵⁰, but here we demonstrate that human networks can revive the oscillations spontaneously. In addition, they revive the oscillations into the stable vortex state as indicated by the vortex order which jumps to $n = 1$ when the oscillations revive.

Violin players can adjust not just the phase and tempo but also their playing amplitude. In highly frustrating situations one or more of the players can reduce their amplitude significantly, known as amplitude death⁵⁰. Representative measurements of such amplitude death are shown in Fig. 5b. Here, the coupling delay of four violin players is increased until one of the players, denoted as Player 1, cannot synchronize with Player 4 leading to frustration. Therefore, this player stops playing, as evidenced by its nearly vanishing amplitude, shown in

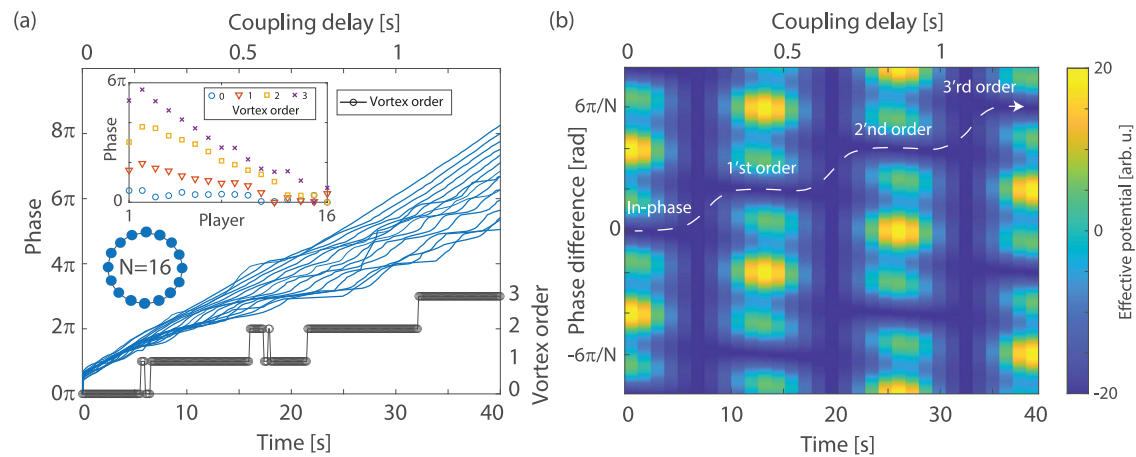


Fig. 3 | Coupled $N=16$ players situated on a ring in a unidirectional coupling, according to the inset scheme, showing spreading of the phase and reaching high order vortex states. a The measured phase of $N=16$ coupled violin players together with the vortex order of the network as we increase the delay of the

coupling between them, showing higher-order vortex states. (Inset) the phase of the 16 players at $t=1.5, 13.5, 24,$ and 34 s, with vortex order $n=0, 1, 2,$ and 3 , respectively. **b** The effective potential of the system as a function of time and coupling delay shows how the system evolves.

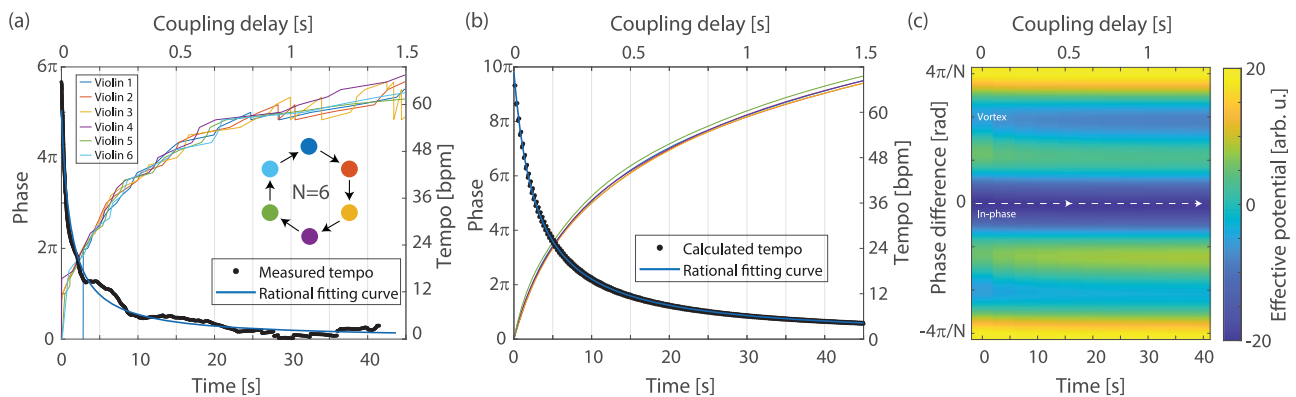


Fig. 4 | Coupled $N=6$ players situated on a ring in a unidirectional coupling showing tempo slowing down. a Experimental measurements of the phase and average tempo as we increase the delayed coupling between them. Each color denotes the phase of a player according to the inset scheme. **b** Numerical

calculations of the system. **c** The effective potential of the system as a function of time when the tempo of the players is following Eq. (5) indicating that the in-phase state stays the global minima for arbitrary large delays.

the lower graph in Fig. 5b. During this time, the player did produce some noise, but no notes were detected. When one of the players stops playing, the closed ring switches into an open ring topology where all the other players are free to shift their phases according to the coupling delay. In an open ring, the players are not limited by the periodic boundary conditions, so the network is stable for any value of delay. After a few seconds, they find the first-order vortex state, and Player 1 resumes playing.

Discussion

To conclude, we investigated the synchronization dynamics of coupled violin players with ring configuration and unidirectional time-delayed coupling. This configuration is governed by a potential landscape that includes well-defined local and global minima that are controlled by the coupling delay time. By starting with a zero coupling delay, we prepared the system in a stable in-phase synchronization state and then adiabatically increased the coupling delay such that the in-phase state became a local minimum. We observed four different routes for the system to escape this local minimum into the global one. We focus on network motifs with global frustration where the

frustration rises from the topology of the network, instead of a local frustration where a node has contradicting inputs.

In the first route, the players change their coupling strength and shift from the local minimum of the in-phase state into the stable vortex state. In the second route, the player slows down their tempo so the in-phase state remains the global minimum. In the third route, all the players play the same note indefinitely which is a stable state regardless of the coupling delay. In the fourth route, one of the players stops playing, effectively changing the system topology into an open ring, thus allowing the players to find the vortex state, and then resume playing.

Our results indicate that human networks are more robust than other networks since they have unique methods for escaping local minima. The results shed new light on the dynamics of human networks and how a group of humans can reach synchronization while escaping local minima. Our investigation offers insights that extend beyond the immediate domain of network dynamics. While our study focuses on the specific context of human interactions modeled through coupled violin players, the principles and mechanisms uncovered have broader implications across multiple disciplines.

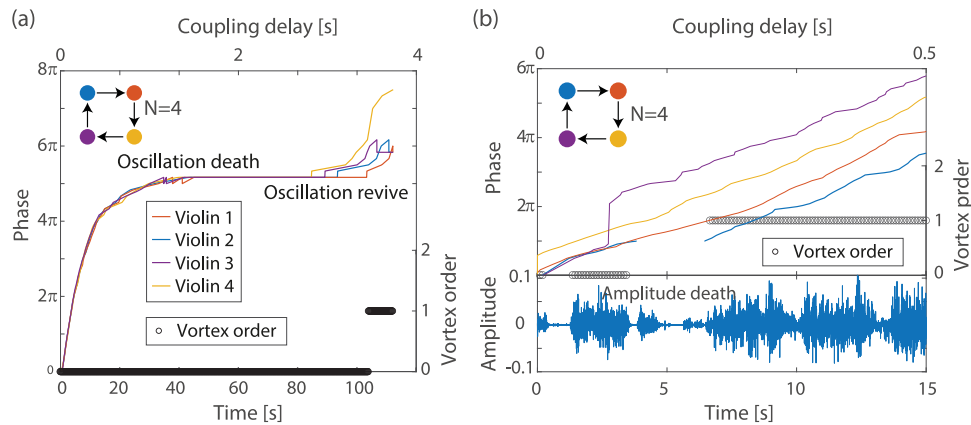


Fig. 5 | Coupled $N = 4$ players situated on a ring in a unidirectional coupling showing oscillation and amplitude death. **a** Coupled violin players reach a state of oscillation death. The players slow down their tempo until all the players play the same note. After 20 seconds, the players revive the oscillation spontaneously into a vortex state. Each color denotes the phase of a player according to the inset

scheme. **b** Coupled violin players show the amplitude death of one player. The upper graph shows the phase of all the players together with the vortex order as a function of time. The lower graph shows the playing amplitude of Player 1 as a function of time. We see that Player 1 stops playing around $t = 5$ s until the system finds the stable first-order vortex state.

In the realm of decision-making theory, our findings highlight the adaptability and resilience of human networks in navigating complex environments. By elucidating the strategies employed by individuals to escape local minima and reach global synchronization states, our research provides valuable insights into the dynamics of group decision-making processes. Understanding these dynamics is crucial in fields such as organizational behavior, management, and policy-making, where the coordination of ideas and actions among individuals is central to achieving collective goals^{34–37}. Moreover, our study has implications for political and economic systems, where the dynamics of human networks play a pivotal role in shaping outcomes. By uncovering how network topology and individual behaviors influence synchronization dynamics, our research offers potential insights into the emergence of leadership, the formation of alliances, and the spread of information within political and economic networks. These insights may inform strategies for enhancing collaboration, fostering innovation, and promoting stability within these systems.

Furthermore, our study has implications for artificial intelligence and machine learning, particularly in the development of algorithms and models that mimic or interact with human networks. By elucidating the dynamics of human interactions and the strategies employed to navigate complex network landscapes, our research may inspire new approaches for designing adaptive and resilient artificial systems capable of learning from and interacting with human networks more effectively.

The Synchronization of periodic motion, generally described by the celebrated Kuramoto model, has a direct mathematical mapping onto the coordinated directional alignment of aperiodic systems⁵¹. These mappings imply that our research on the synchronization of periodic behavior can be applied to a variety of coordinated aperiodic behaviors in humans, animals, and physical systems^{25,52}.

An exciting extension of our research is to incorporate real-time analysis of the network and detect the different connections. This will enable us to experiment and study dynamical networks, where the parameters of the networks change according to the state of synchronization between the nodes. With this system, we will study how leaders are formed in a human network and if it is possible to control who will become a leader and who will become a follower.

Methods

Our system is based on coupling 16 violin players connected via a computer system. We record the output from each violin with a pickup

microphone (Barcus-Berry True Expression Violin Piezo Pickup). These pickup microphones are connected with a 10 m cables to a sound card (Focusrite Scarlett 18i20) and to an optical extension (Focusrite Scarlett OctoPre Dynamic). The sound cards are connected to a computer (MacBook Pro M3) that controls on the input and decides which channel is connected to which. The output is directed from the computer through the sound card and 10 m cables to professional sound isolation earphones (Shure Se 215).

In order to analyze the result, we use a note detection program that analyzes the output from each violin and writes it in a *.wav file. From this file, we obtain the phase of each player as a function of time. We include the delay between each player and the connectivity of the network to find which player is following which. This allows us to analyze when the system is leaving the in-phase state of synchronization and reaching the vortex state of synchronization. We numerically calculate the derivative of the phase as a function of time to obtain the tempo of each player. Finally, we analyze the amplitude of each player to identify when each player stopped playing. All the code used to obtain and analyze the results is available online. All players agreed to the use of the data in this study.

Data availability

All the raw measured data generated in this study have been deposited in the figshare database under accession code CC BY 4.0: https://figshare.com/projects/local_minima_in_human_networks/167306.

Code availability

All the code developed for gathering the data and for analyzing the data in this study has been deposited in the figshare database under accession code CC BY 4.0: https://figshare.com/projects/local_minima_in_human_networks/167306.

References

- Néda, Z., Ravasz, E., Brechet, Y., Vicsek, T. & Barabási, A.-L. Self-organizing processes: The sound of many hands clapping. *Nature* **403**, 849 (2000).
- Strogatz, S. H., Abrams, D. M., McRobie, A., Eckhardt, B. & Ott, E. Theoretical mechanics: Crowd synchrony on the millennium bridge. *Nature* **438**, 43 (2005).
- Javarone, M. A. & Marinazzo, D. Evolutionary dynamics of group formation. *PLoS ONE* **12**, 0187960 (2017).

4. Werner, B. & Mcnamara, D. E. Dynamics of coupled human-landscape systems. *Geomorphology* **91**, 393–407 (2007).
5. Sumpter, D. J., Zabzina, N. & Nocolis, S. C. Six predictions about the decision making of animal and human groups. *Manag. Decis. Econ.* **33**, 295–309 (2012).
6. Smaldino, P. E. & Richerson, P. J. The origins of options. *Front. Neurosci.* **6**, 50 (2012).
7. Wasserman, S. & Faust, K. *Social Network Analysis: Methods And Applications*. Vol. 8 (Cambridge University Press, 1994)
8. Morris, M. E. Social networks as health feedback displays. *IEEE Internet Comput.* **9**, 29–37 (2005).
9. Solferino, N. & Tessitore, M. E. Human networks and toxic relationships. *Mathematics* **9**, 2258 (2021).
10. Sumpter, D. J. The principles of collective animal behaviour. *Philos. Trans. R. Soc. Lond. B Biol. Sci.* **361**, 5–22 (2006).
11. Sarfati, R. & Peleg, O. Chimera states among synchronous fireflies. *Sci. Adv.* **8**, 6690 (2022).
12. Davis, P. K., Ho, A. & Dowdy, S. F. Biological methods for cell-cycle synchronization of mammalian cells. *Biotechniques* **30**, 1322–1331 (2001).
13. Dörfler, F. & Bullo, F. Synchronization in complex networks of phase oscillators: a survey. *Automatica* **50**, 1539–1564 (2014).
14. Calabrese, C. et al. Spontaneous emergence of leadership patterns drives synchronization in complex human networks. *Sci. Rep.* **11**, 18379 (2021).
15. Conradt, L. & Roper, T. J. Consensus decision making in animals. *Trends Ecol. Evol.* **20**, 449–456 (2005).
16. Gambuzza, L. V. et al. Stability of synchronization in simplicial complexes. *Nat. Commun.* **12**, 1255 (2021).
17. Sorrentino, F., Barlev, G., Cohen, A. B. & Ott, E. The stability of adaptive synchronization of chaotic systems. *Chaos: Interdiscip. J. Nonlinear Sci.* **20**, 013103 (2010).
18. Kassabov, M., Strogatz, S. H. & Townsend, A. A global synchronization theorem for oscillators on a random graph. *Chaos: Interdiscip. J. Nonlinear Sci.* **32**, 093119 (2022).
19. Roy, R., Murphy Jr, T., Maier, T., Gills, Z. & Hunt, E. Dynamical control of a chaotic laser: experimental stabilization of a globally coupled system. *Phys. Rev. Lett.* **68**, 1259 (1992).
20. Fridman, M., Nixon, M., Davidson, N. & Friesem, A. A. Passive phase locking of 25 fiber lasers. *Opt. Lett.* **35**, 1434–1436 (2010).
21. Ling, S., Xu, R. & Bandeira, A. S. On the landscape of synchronization networks: a perspective from nonconvex optimization. *SIAM J. Optim.* **29**, 1879–1907 (2019).
22. Ravoori, B. et al. Robustness of optimal synchronization in real networks. *Phys. Rev. Lett.* **107**, 034102 (2011).
23. Leylaz, G., Wang, S. & Sun, J.-Q. Identification of nonlinear dynamical systems with time delay. *Int. J. Dyn. Control* **10**, 1–12 (2021).
24. Fridman, M., Pugatch, R., Nixon, M., Friesem, A. A. & Davidson, N. Measuring maximal eigenvalue distribution of wishart random matrices with coupled lasers. *Phys. Rev. E* **85**, 020101 (2012).
25. Feinerman, O., Pinkoviezky, I., Gelblum, A., Fonio, E. & Gov, N. S. The physics of cooperative transport in groups of ants. *Nat. Phys.* **14**, 683–693 (2018).
26. Pal, V., Tradonsky, C., Chriki, R., Friesem, A. A. & Davidson, N. Observing dissipative topological defects with coupled lasers. *Phys. Rev. Lett.* **119**, 013902 (2017).
27. Kawaguchi, K. Deep learning without poor local minima. Advances in neural information processing systems. *arXiv* <https://doi.org/10.48550/arXiv.1605.07110> (2016).
28. Ayodele, T. O. Types of machine learning algorithms. *N. Adv. Mach. Learn.* **3**, 19–48 (2010).
29. Jalan, S., Amritkar, R. & Hu, C.-K. Synchronized clusters in coupled map networks. i. numerical studies. *Phys. Rev. E* **72**, 016211 (2005).
30. Heim, B., Rønnow, T. F., Isakov, S. V. & Troyer, M. Quantum versus classical annealing of ising spin glasses. *Science* **348**, 215–217 (2015).
31. Shahal, S. et al. Synchronization of complex human networks. *Nat. Commun.* **11**, 3854 (2020).
32. Antonioni, A. & Cardillo, A. Coevolution of synchronization and cooperation in costly networked interactions. *Phys. Rev. Lett.* **118**, 238301 (2017).
33. D’Ausilio, A., Novembre, G., Fadiga, L. & Keller, P. E. What can music tell us about social interaction? *Trends Cogn. Sci.* **19**, 111–114 (2015).
34. Wiseman, A. W. & Davidson, P. M. *The Rhythmic Application Of Evidence-based Policy In National Educational Systems Worldwide*. p. 1–17 (Emerald Publishing Limited, 2018).
35. Koehler, G. Time, complex systems, and public policy: a theoretical foundation for adaptive policy making. *Nonlinear Dyn. Psychol. Life Sci.* **7**, 99–114 (2003).
36. Morçöl, G. *A Complexity Theory For Public Policy* (Routledge, 2013)
37. Hawe, P., Shiell, A. & Riley, T. Theorising interventions as events in systems. *Am. J. Community Psychol.* **43**, 267–276 (2009).
38. Tradonsky, C. et al. Conversion of out-of-phase to in-phase order in coupled laser arrays with second harmonics. *Photon. Res.* **3**, 77–81 (2015).
39. Pal, V. et al. Phase locking of even and odd number of lasers on a ring geometry: effects of topological-charge. *Opt. Express* **23**, 13041–13050 (2015).
40. Kolling, A., Walker, P., Chakraborty, N., Sycara, K. & Lewis, M. Human interaction with robot swarms: a survey. *IEEE Trans. Hum.-Mach. Syst.* **46**, 9–26 (2015).
41. Alon, U. Network motifs: theory and experimental approaches. *Nat. Rev. Genet.* **8**, 450–461 (2007).
42. Kashtan, N., Itzkovitz, S., Milo, R. & Alon, U. Topological generalizations of network motifs. *Phys. Rev. E* **70**, 031909 (2004).
43. Roy, S., Ghosh, P., Barua, D. & Das, S. K. Motifs enable communication efficiency and fault-tolerance in transcriptional networks. *Sci. Rep.* **10**, 9628 (2020).
44. Stone, L., Simberloff, D. & Artzy-Randrup, Y. Network motifs and their origins. *PLoS Comput. Biol.* **15**, 1006749 (2019).
45. Kuramoto, Y. *Chemical Oscillations, Waves, And Turbulence*. Vol. 19 (Springer, 2012).
46. Kuramoto, Y. & Nishikawa, I. Statistical macrodynamics of large dynamical systems. case of a phase transition in oscillator communities. *J. Stat. Phys.* **49**, 569–605 (1987).
47. Strogatz, S. H. From Kuramoto to Crawford: exploring the onset of synchronization in populations of coupled oscillators. *Phys. D Nonlinear Phenom.* **143**, 1–20 (2000).
48. Ermentrout, G. B. Oscillator death in populations of “all to all” coupled nonlinear oscillators. *Phys. D Nonlinear Phenom.* **41**, 219–231 (1990).
49. Chafe, C., Caceres, J.-P. & Gurevich, M. Effect of temporal separation on synchronization in rhythmic performance. *Perception* **39**, 982–992 (2010).
50. Zou, W., Senthilkumar, D., Koseska, A. & Kurths, J. Generalizing the transition from amplitude to oscillation death in coupled oscillators. *Phys. Rev. E* **88**, 050901 (2013).
51. Nixon, M., Ronen, E., Friesem, A. A. & Davidson, N. Observing geometric frustration with thousands of coupled lasers. *Phys. Rev. Lett.* **110**, 184102 (2013).
52. Gelblum, A. et al. Ant groups optimally amplify the effect of transiently informed individuals. *Nat. Commun.* **6**, 7729 (2015).

Acknowledgements

The authors would like to thank Prof. Yuval Garini and Tal Yizreal and the Fetter Museum of Nanoscience and Art at Bar-Ilan University for establishing the collaboration; Transmeet Art and Science Festival and the Steinhart Museum of Natural History for hosting the art event; Amir Bolzman and Lars Sargel for being the sound engineers; Prof. Ofer Feinerman for fruitful discussions; and funding by the Yeda-Sela Foundation.

Author contributions

E.S, N.D., and M.F. conceived the experiments, E.S, H.D., and M.F. designed the experiments, E.S designed the computer code, E.S, Y.A., and S.S. conducted the experiments, and E.S and M.F. analyzed the results. E.S. and M.F. wrote the manuscript. All authors reviewed the manuscript.

Competing interests

The authors declare no competing interests.

Additional information

Supplementary information The online version contains supplementary material available at <https://doi.org/10.1038/s41467-024-53540-7>.

Correspondence and requests for materials should be addressed to Moti Fridman.

Peer review information *Nature Communications* thanks the anonymous reviewers for their contribution to the peer review of this work. A peer review file is available.

Reprints and permissions information is available at <http://www.nature.com/reprints>

Publisher's note Springer Nature remains neutral with regard to jurisdictional claims in published maps and institutional affiliations.

Open Access This article is licensed under a Creative Commons Attribution-NonCommercial-NoDerivatives 4.0 International License, which permits any non-commercial use, sharing, distribution and reproduction in any medium or format, as long as you give appropriate credit to the original author(s) and the source, provide a link to the Creative Commons licence, and indicate if you modified the licensed material. You do not have permission under this licence to share adapted material derived from this article or parts of it. The images or other third party material in this article are included in the article's Creative Commons licence, unless indicated otherwise in a credit line to the material. If material is not included in the article's Creative Commons licence and your intended use is not permitted by statutory regulation or exceeds the permitted use, you will need to obtain permission directly from the copyright holder. To view a copy of this licence, visit <http://creativecommons.org/licenses/by-nc-nd/4.0/>.

© The Author(s) 2024